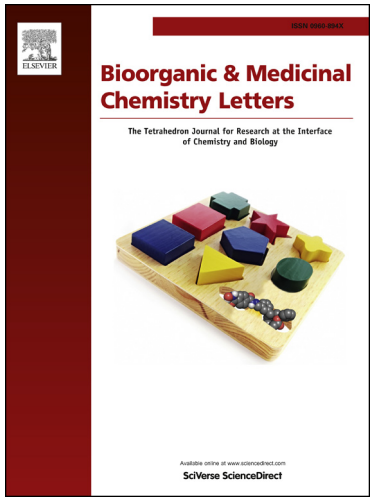

Scaffold hopping approach towards various AFQ-056 analogs as potent metabotropic glutamate receptor 5 negative allosteric modulators

Holger Kubas, Udo Meyer, Mirko Hechenberger, Kai-Uwe Klein, Patrick Plitt, Ronalds Zemribo, Harm W. Spexgoor, Sander G.A. van Assema, Ulrich Abel

PII: S0960-894X(13)01133-5
DOI: http://dx.doi.org/10.1016/j.bmcl.2013.09.059
Reference: BMCL 20911

To appear in: *Bioorganic & Medicinal Chemistry Letters*

Received Date: 19 August 2013
Revised Date: 17 September 2013
Accepted Date: 21 September 2013

Please cite this article as: Kubas, H., Meyer, U., Hechenberger, M., Klein, K-U., Plitt, P., Zemribo, R., Spexgoor, H.W., van Assema, S.G.A., Abel, U., Scaffold hopping approach towards various AFQ-056 analogs as potent metabotropic glutamate receptor 5 negative allosteric modulators, *Bioorganic & Medicinal Chemistry Letters* (2013), doi: http://dx.doi.org/10.1016/j.bmcl.2013.09.059

Graphical Abstract

Scaffold hopping approach towards various AFQ-056 analogs as potent metabotropic glutamate receptor 5 negative allosteric modulators

Leave this area blank for abstract info.

Holger Kubas[a], Udo Meyer[a], Mirko Hechenberger[a], Kai-Uwe Klein[a], Patrick Plitt[a], Ronalds Zemribo[b], Harm W. Spexgoor[c], Sander G.A. van Assema[c], and Ulrich Abel[a]

[a] *Merz Pharmaceuticals GmbH, Eckenheimer Landstrasse 100, 60318 Frankfurt am Main, Germany*

[b] *Institute of Organic Synthesis, Aizkraukles iela 21, Riga, LV1006, Latvia*

[c] *Mercachem B.V., Kerkenbos 1013, 6546 BB Nijmegen, The Netherlands*

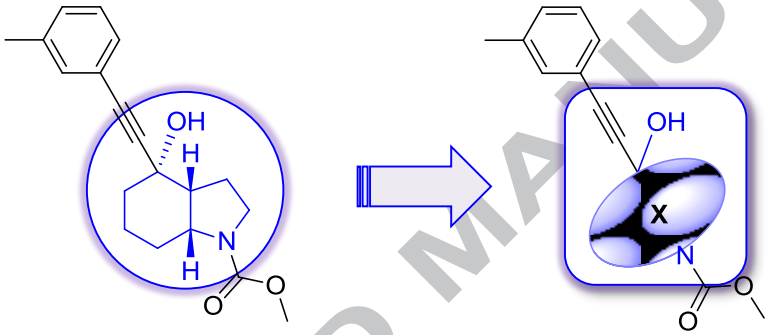

AFQ-056
(Novartis)

X = 18 different core structures

Bioorganic & Medicinal Chemistry Letters
journal homepage: www.elsevier.com

Scaffold hopping approach towards various AFQ-056 analogs as potent metabotropic glutamate receptor 5 negative allosteric modulators

Holger Kubas[a,*], Udo Meyer[a], Mirko Hechenberger[a], Kai-Uwe Klein[a], Patrick Plitt[a], Ronalds Zemribo[b], Harm W. Spexgoor[c], Sander G.A. van Assema[c], and Ulrich Abel[a]

[a] *Merz Pharmaceuticals GmbH, Eckenheimer Landstrasse 100, 60318 Frankfurt am Main, Germany*
[b] *Institute of Organic Synthesis, Aizkraukles iela 21, Riga, LV1006, Latvia*
[c] *Mercachem B.V., Kerkenbos 1013, 6546 BB Nijmegen, The Netherlands*

ARTICLE INFO

Article history:
Received
Revised
Accepted
Available online

Keywords:
Metabotropic glutamate receptor
mGluR5
Allosteric modulator
Scaffold hopping
AFQ-056

ABSTRACT

The metabotropic glutamate receptor subtype 5 has evolved into a promising target for the treatment of various diseases of the central nervous system, such as Fragile X and L-DOPA induced dyskinesia. One of the most advanced clinical compound is Novartis' AFQ-056 (Mavoglurant), which served us as a template for a scaffold hopping approach, generating a structurally diverse set of potent analogs. Both the limited aqueous solubility and the relatively poor metabolic stability of AFQ-056 were improved with hexahydrocyclopenta[*c*]pyrrole derivative **54a**, which proved to be a valuable candidate for further development.

Glutamate is the most prominent excitatory neurotransmitter in the brain and crucial for memory formation, regulation, and learning.[1] It functions via ionotropic glutamate receptors and via G-protein coupled metabotropic glutamate receptors (mGluR), which belong to the GPCR family C. mGluR5 together with mGluR1 belongs to the group I of mGluRs. It is centrally expressed in the limbic cortex, hippocampus, amygdala, basal ganglia, and thalamus, as well as peripherally in the skin and the vagal nerve system,[2] which reflects the multitude of pharmacological effects anticipated for mGluR5 modulators. As a classical mGlu receptor, the mGluR5 is structurally composed of a large extracellular N-terminal domain, which harbors the orthosteric binding site, and of a seven transmembrane (7TM) α-helical domain, which accommodates the allosteric MPEP binding site.[3] It couples positively to phospholipase C via G_q, eventually leading to an increase of intracellular calcium.[4] Orthosteric inhibitors of mGluR5 were shown to be of limited use as leads for drug discovery as a consequence of their high compound polarity, poor bioavailability and a low brain penetration. In contrast, negative allosteric modulators (NAMs) are in general more lipophilic, and mGluR5 NAMs were shown to exhibit properties, which are in accordance with the use as CNS-acting compounds. Since NAMs exert their modulatory effect in a non-competitive way, the tempo-spatial signaling pattern of endogenous glutamate is maintained and modulated rather than being fully suppressed.

mGluR5 NAMs have been clinically tested in Fragile-X syndrome (FXS),[5] anxiety,[2] L-DOPA induced dyskinesia (LID),[6] gastro-esophageal reflux disease (GERD),[7] migraine,[8] and chorea in Huntington´s disease.[9] The most advanced clinical candidate is Novartis´ Mavoglurant (AFQ-056, **1**), which is currently being tested in in a phase 3 clinical trial for the treatment of FXS,[10] and which has also successfully been evaluated in phase 2 clinical trials for LID, similarly to Addex´ Dipraglurant (ADX48621, **2**)[11] and Roche´s RG-7090 (**3**)[11, 12] (Figure 1). However, no marketed mGluR5 drug has yet evolved, and there is a continuing demand of additional chemical lead structures.

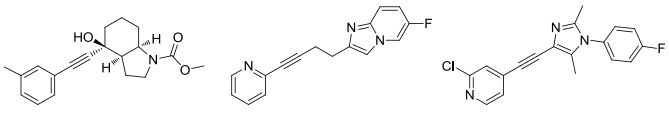

Figure 1. Clinically evaluated mGluR5 negative allosteric modulators.

We here describe the discovery and optimization of novel potent acetylenic mGluR5 negative allosteric modulators based on the chemical structure of Novartis' drug candidate AFQ-056 (**1**). In contrast to most of the published mGluR5 NAMs

* Corresponding author. Tel.: +49-(0)69-1503-478; fax: +49-(0)69-1503-188; e-mail: holger.kubas@merz.de, hkubas@freenet.de

containing a triple bond motif, the bicyclic scaffold presents a relatively high fraction of sp^3 hybridized carbons (Fsp^3), which is often associated with a superior drug-like profile as compared with 'flat' diarylalkynes.[13] Several molecular parameters crucial for a successful development of an oral drug, such as aqueous solubility and selectivity over relevant off-targets, are supposed to be significantly improved by adding three-dimensionality to the molecular structure. Therefore, the fully saturated bicyclic core of **1** was chosen as a template for a scaffold-hopping approach, resulting in the identification of various nitrogen-containing bicyclic and spiro ring systems. The first hit series around compound **9** was further varied at three different positions to examine structure-activity-relationships. For all other identified scaffolds the substitution pattern of AFQ-056 was maintained to enable a proper comparison with the original. As a result, seven out of the 18 novel scaffold series produced compounds with *in vitro* activities in the low nanomolar range (IC_{50} < 100 nM).

At first, a diverse set of nortropane-related analogs of compound **1** was prepared as outlined in Schemes 1–3, starting with nortropinone hydrochloride.[14] Final products **5**–**10**, **11a**, **11b**, and **12** were prepared in two steps. The starting material was first treated with methyl chloroformate in the presence of triethylamine and DMAP to form the carbamate intermediate **4** (Scheme 1). In a subsequent step, an appropriate ethynylbenzene was first deprotonated by means of *n*-butyllithium (*n*-BuLi) and then reacted with ketone **4** to provide the target compounds.

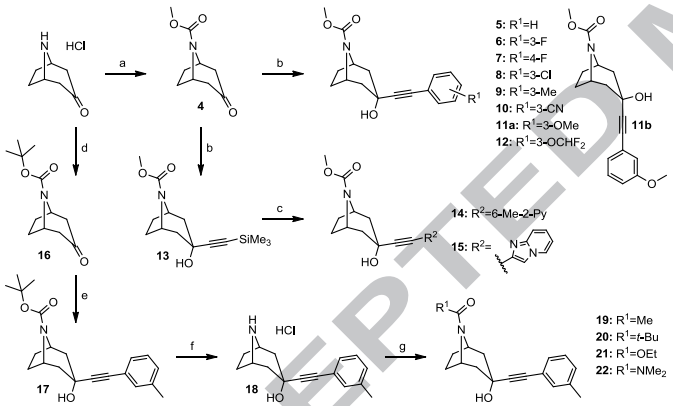

Scheme 1. Reagents and conditions: (a) methyl chloroformate, Et_3N, DMAP, THF, rt, 3 h; (b) 1. subst. ethyne, *n*-BuLi, THF, -20 °C → 0 °C, 90 min; 2. **4**, THF, -78 °C → 0–5 °C, 2 h; (c) aryl halide, Et_3N, DMF, CuI, $PdCl_2(PPh_3)_2$, TBAF, THF, 60 °C, 2 h → rt, overnight; (d) di-*tert*-butyl dicarbonate, Et_3N, DMAP, DCM, 0 °C → rt, 16 h; (e) 1. 1-ethynyl-3-methylbenzene, *n*-BuLi, THF, -20 °C → 0 °C, 1 h; 2. **16**, THF, -20 °C → 0 °C; 1h; (f) 4N HCl in dioxane, DCM, rt, 1h; (g) R-C(O)Cl, Et_3N, DCM, 0 °C → rt, overnight.

Basically, the ethinylation of nortropinone derivatives could produce two different isomers, *endo* or *exo*, depending on the side of attack of the alkyne anion. The crystal structure of a representative derivative (**I**, Figure 2) confirmed our presumption that the *endo*-OH orientation was the favored stereoconfiguration of the final products. However, in a few cases both isomers were formed and isolated (see methoxy derivatives **11a** and **11b**).

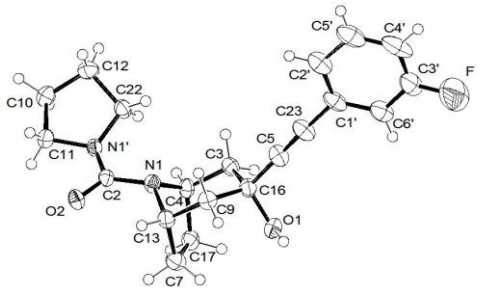

Figure 2. Crystal structure of 3-((3-fluorophenyl)ethynyl)-3-*endo*-hydroxy-8-azabicyclo[3.2.1]octan-8-yl)(pyrrolidin-1-yl)methanone (**I**).

Final compounds **14** and **15**, containing a heteroaryl residue, were also synthetically accessible via intermediate product **4**, which was treated with ethynyltrimethylsilane to yield alkyne **13** (Scheme 1). The TMS group was finally replaced by an appropriate aryl halide using tetrabutylammonium fluoride (TBAF), a suitable palladium catalyst, and copper(I)iodide under basic conditions, leading to the formation of the desired products. *N*-Derivatized compounds **19**–**22** were made via Boc-protected intermediate **16**, which was synthesized from nortropinone employing di-*tert*-butyl dicarbonate under basic conditions. Ketone **16** was then reacted with 1-ethynyl-3-methylbenzene in the presence of *n*-BuLi to give alkyne derivative **17**, which was subsequently *N*-deprotected using hydrochloric acid. In the last step, the formed cyclic amine (as HCl salt) was converted into the final products via coupling reactions with an appropriate acyl chloride, ethyl chloroformate, or dimethylcarbamoyl chloride, respectively (Scheme 1).

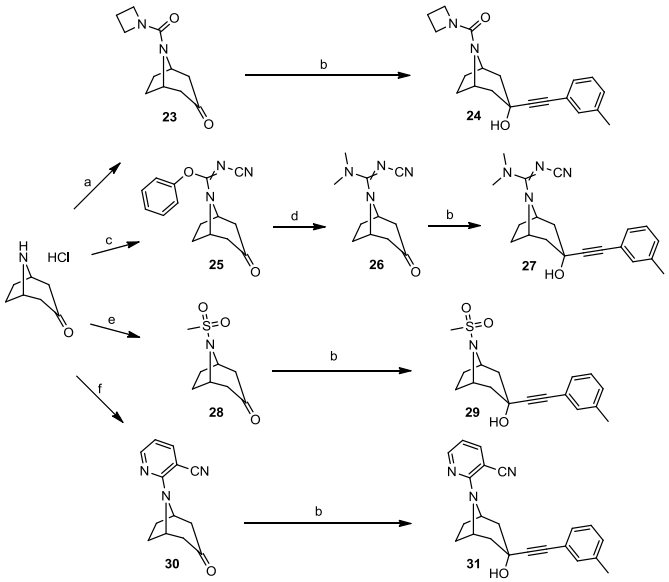

Scheme 2. Reagents and conditions: (a) 1. diphosgene, DCM, rt, 30 min; 2. azetidine, Et_3N, rt, 1 h; (b) 1. 1-ethynyl-3-methylbenzene, *n*-BuLi, THF, -20 °C → 0 °C, 90 min; 2. **23**, **26**, **28**, or **30**, resp., THF, -78 °C → 0–5 °C, 2 h; (c) diphenyl cyanocarbonimidate, Et_3N, DCM, rt, 2 h; (d) Et_2NH/THF, iPrOH, 80 °C, 3 h; (e) methylsulfonyl chloride, DIPEA, DCM, rt, 4 h; (f) 2-chloronicotinonitrile, Et_3N, THF, reflux, 3 days.

The synthesis routes towards additional, diversely *N*-substituted products **24**, **27**, **29**, and **31** are depicted in Scheme 2. The respective precursors were made from nortropinone hydrochloride. Intermediate **23** was formed in a one-pot-two-step reaction using diphosgene and azetidine. Diphenyl cyanocarbonimidate was employed to prepare **25**, which was then further reacted with diethylamine to give cyanoguanidine derivative **26**. *N*-Sulfonyl analog **28** was synthesized using methylsulfonyl chloride, and *N*-arylation of the starting material with 2-chloronicotinonitrile yielded precursor **30**. Ultimately, the four intermediate ketones were treated with deprotonated 1-ethynyl-3-methylbenzene to provide the final products, as described above.

Introduction of a hydrogen atom in 3-position turned out to be rather challenging. Eventually, a 4-step-procedure successfully provided compound **35** (Scheme 3). The synthesis route started from ketone **4**, which was converted to spiro oxirane derivative **32** using trimethylsulfoxonium iodide and potassium *tert*-butoxide as base. The formed epoxide ring was opened up by means of boron trifluoride etherate, and subsequent treatment with DBU in methanol gave exocyclic ketone **33**, which was then further reacted to alkyne **34** by applying Bestmann-Ohira conditions.[15] Finally, the *m*-tolyl residue was appended via a Sonogashira reaction using 1-iodo-3-methylbenzene in the presence of a suitable palladium catalyst and copper(I)iodide under basic conditions to furnish product **35**.[16] 3-Methoxy analog **36** was prepared by *O*-methylation of compound **9** with methyl iodide and *n*-BuLi under cryogenic conditions (Scheme 3).

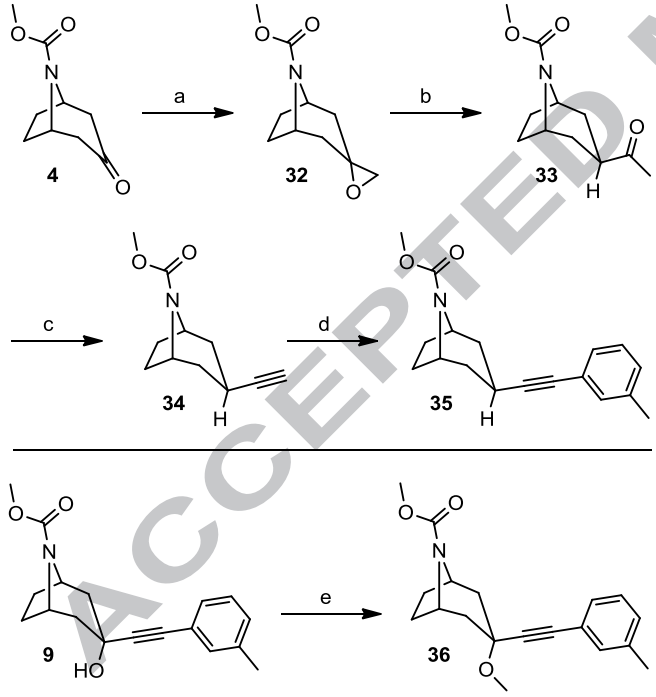

Scheme 3. Reagents and conditions: (a) 1. trimethylsulfoxonium iodide, KO*t*Bu, THF, N_2, reflux, 3 h; 2. **4**, THF, rt, 3 days; (b) 1. **32**, $BF_3{\times}Et_2O$, THF, -3 °C → 5 °C; 3 h, rt, overnight; 2. DBU, MeOH, THF, rt, 1 h; (c) dimethyl 1-diazo-2-oxopropylphosphonate, K_2CO_3, MeOH, 0 °C → rt, 2 h; (d) 1-iodo-3-methylbenzene, $Pd(PPh_3)_4$, CuI, Et_3N, DMF, N_2, 60 °C, 1 h; (e) *n*-BuLi (1.6M in hexanes), MeI, THF, DMSO, -78 °C, 1.5 h.

Preparation of a set of compounds containing various bicyclic core structures is generically described in Scheme 4 (details are given in the Supplementary data). Boc-protected amines were directly treated with deprotonated 1-ethynyl-3-methylbenzene. Subsequent steps included *N*-deprotection and conversion to the final product by treating the amine with ethyl chloroformate. Alternatively, the starting material was first deprotected, followed by conversion to the corresponding methyl carbamate, which was finally subjected to the ethinylation reaction described above. Respective *N*-benzylated building blocks – either commercially available or synthesized from suitable precursors – were converted to the corresponding carbamates either directly or in a two-step-procedure via the amine intermediate. Final ethinylation was performed according to the previously delineated procedure.

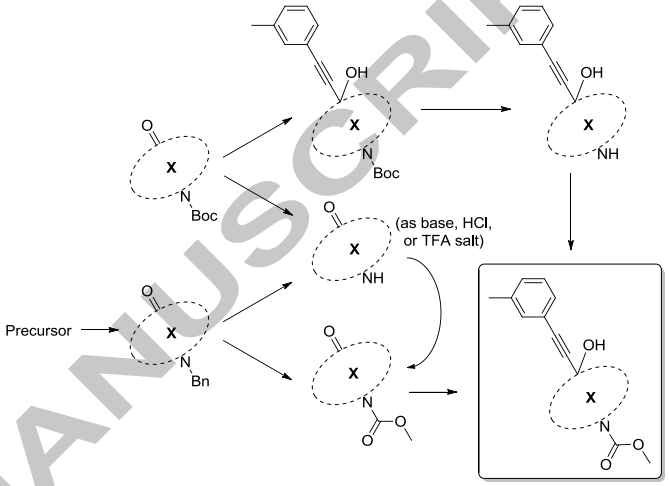

Scheme 4. General synthesis routes towards final products **39**, **42**, **45**, **47**, **49**, **52a**, **52b**, **54**, **54a**, **54b**, **57**, **60**, **62**, **65**, **68**, **70**, **70a**, **70b**, **74**, **76**, **79**, **82**, **85**, and **87**. For details please refer to the Supplementary data.

Each of the synthesized compounds was tested in a functional assay to determine the activity on the human mGlu5 receptor stably expressed in CHO cells. The assay was based on the detection of intracellularly mobilized calcium using a calcium sensitive dye. For all compounds which were found to be active (%inhibition >50%) at 10 µM test concentration follow-up measurements were performed in form of concentration response curves to examine their functional potencies. Most active compounds were further characterized in rat primary astrocytes, whereby their mGluR5 NAM activities could be demonstrated also in native tissue.

In general, the *in vitro* potencies determined in primary cells (rat primary astrocytes) were found to be in very good agreement with those obtained from CHO cells containing the human mGlu5 receptor. Moreover, the high affinities of several compounds tested in a binding assay (replacement of [^{3}H]-M-MPEP) proved our assumption that this type of mGluR5 ligands binds to the MPEP allosteric site (Table 1). All tested compounds were found to be highly selective over the mGlu1 receptor (data not shown).

Detailed structure-activity relationships of the synthesized tropinone derivatives are summarized in Table 1. Within the first set of ten compounds the residue R^2 was systematically modified, while the methoxycarbonyl group as *N*-substituent (R^1) and the hydroxyl group as residue R^3 were retained. The prototypic derivative **5** bearing an unsubstituted phenyl ring already showed moderate to good activity with an IC_{50} value at the human mGlu5 receptor of 0.298 µM. Moreover, the *in vitro* potency could be substantially elevated by adding a substituent to the 3-position, demonstrated by compounds **6** (3-F, 5-fold increase), **8** (3-Cl, 10-

fold), the direct AFQ-056 analog **9** (3-Me, 6-fold), **10** (3-CN, 2-fold), **11a** (3-OMe, 4-fold), and **12** (3-$OCHF_2$, 4-fold). In contrast, substitution in 4-position (compound **7**, 4-F, IC_{50} = 2.19 µM) and replacement of the benzene ring by pyridine (compound **14**, IC_{50} = 0.818 µM) led to a marked drop of activity. Further variations of the pyridine residue like bicyclic heteroaryl ring systems turned out to be even more detrimental, exemplified by the inactive imidazopyridine derivative **15**. Notably, the isolated *exo*-OH isomer of **11a**, this is **11b** (see Scheme 1), was found to be active only in the micromolar range (data not shown), providing evidence that the *endo*-configuration is clearly favored.

In a second step, the *N*-substitution (R^1) was varied, keeping the original R^2 (*m*-tolyl) and R^3 (OH) residues of parent compound **1**. Interestingly, the replacement of the *N*-methoxycarbonyl moiety of compound **9** by a simple *n*-propyl group caused a total loss of activity (data not shown). This and the results obtained for *N*-acyl derivatives **19** and **20** revealed that a H-bond acceptor function like a carbonyl group in α-position to the nitrogen seems to be crucial for submicromolar potencies. However, compared to compound **9** these amides were found to be 6- and 10-fold less active, respectively. A series of further amides showed activities in the same range or lower (data not shown). Switching from amide to ethyl carbamate (**21**) restored the 2-digit nanomolar potency of methyl analog **9**. Further variation of the carbamate function yielded reasonably active urea derivatives **22** (hIC_{50} = 0.132 µM) and **24** (hIC_{50} = 0.210 µM). Appending larger azetidine homologs like, for example, a pyrrolidine ring, did not improve the potency of **24** (data not shown). In comparison to the urea derivatives, cyanoguanidine **27** turned out to be equipotent, whereas the activity of the more polar methylsulfonyl analog **29** was ~3-fold lower. Due to the similar potencies found for **29** and its acetyl analog **19** the sulfonyl group presented a suitable bioisoster for C=O. Finally, compound **31**, bearing 3-cyanopyridin-2-yl as an *N*-aryl residue, reached *in vitro* results which were comparable with those obtained for its bioisosteric cyanoguanidine **27**.

A third small series comprised of compounds **34** and **35** demonstrated that the hydroxyl group (R^3) is not mandatory for reaching high potencies. Both a simple hydrogen residue and a methoxy group were shown to be equivalent. However, aqueous solubility was significantly diminished by these modifications (data not shown).

In summary, the *in vitro* activity results obtained for the nortropane series around compound **9** clearly evinced that small changes of the original substitution pattern of AFQ-056 were generally tolerated, indicated by several equipotent compounds such as **6**, **8**, **11a**, **12**, **21**, and **35**. However, more distinct modifications of the functionalities often led to a marked drop of *in vitro* potencies. This finding applied to the change of the position of substitution on the phenyl ring, to the replacement of the phenyl residue by heteroaryl rings, and to specific variations of the *N*-substituent. Moreover, it was figured that the hydroxyl group in 3-position of the bicyclic ring system was not crucial for achieving high activities as shown with compounds **35** and **36**.

Table 1. mGluR5 *in vitro* potency data of azabicyclo[3.2.1]octane derivatives

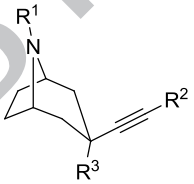

Compound ID	R^1	R^2	R^3	Human mGluR5 (CHO) IC_{50} (µM)[a]	Rat mGluR5 (rpA) IC_{50} (µM)[a]	Rat mGluR5 (ctx) [^{3}H]-M-MPEP K_i (µM)[b]
1 (AFQ-056)	-	-	-	0.0716±0.00647	0.0516±0.00595	0.0660±0.00624
5			OH	0.298±0.0248	Nt	Nt
6		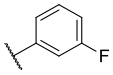	OH	0.0613±0.0091	0.0678±0.00489	0.0777±0.00577
7		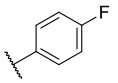	OH	2.19	Nt	Nt
8		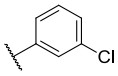	OH	0.0274±0.00296	0.0252	Nt
9		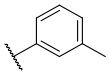	OH	0.0507±0.00579	0.0479±0.00583	0.0710
10		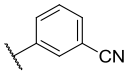	OH	0.187±0.0282	Nt	Nt
11a		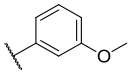	OH	0.0763±0.00877	0.0740	0.0760

12	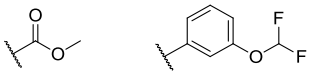		OH	0.0722±0.0142	0.0907	0.0578±0.00612
14			OH	0.818	Nt	Nt
15	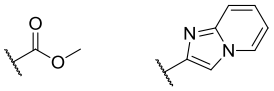		OH	>100	Nt	Nt
19			OH	0.543	Nt	Nt
20			OH	0.308±0.00664	Nt	Nt
21	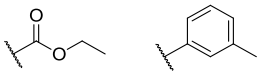		OH	0.0478±0.00247	0.0291	Nt
22			OH	0.132±0.0172	0.113	Nt
24			OH	0.210±0.0219	Nt	Nt
27	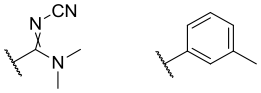		OH	0.168±0.0150	Nt	Nt
29			OH	0.575	Nt	Nt
31	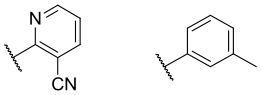		OH	0.170±0.0248	Nt	Nt
35			H	0.0648±0.0140	Nt	Nt
36			OMe	0.137±0.0264	Nt	Nt

[a] IC_{50} values are given as geometric means ±SEM of at least three independent experiments, each performed in quadruplicate (no SEM-values indicate a lower number of independent experiments).

[b] Replacement of [^{3}H]-M-MPEP; K_i values are given as geometric means ±SEM of at least three independent experiments each performed in triplicates.

Table 2. mGluR5 *in vitro* potency data of further AFQ-056 analogs

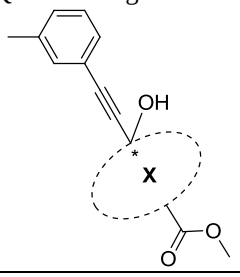

Compound ID	X	Human mGluR5 (CHO) IC_{50} (µM)[a]	Rat mGluR5 (rpA) IC_{50} (µM)[a]	Rat mGluR5 (ctx) [^{3}H]-M-MPEP K_i (µM)[b]

1 (AFQ-056)	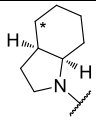	0.0716±0.00647	0.0516±0.00595	0.0660±0.00624
9		0.0507±0.00579	0.0479±0.00583	0.0710
39		1.02	Nt	Nt
42		5.0 (est.)	Nt	Nt
45		49 (est.)	Nt	Nt
47	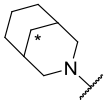	0.0466±0.0055	0.0325	Nt
49	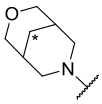	3.35	Nt	Nt
52a (*exo*-OH)		0.0850±0.00613	0.0387	Nt
52b (*endo*-OH)		52 (est.)	Nt	Nt
54 (*rac*)	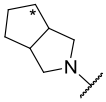	0.103±0.0169	0.188±0.0274	Nt
54a (E1)		0.0748±0.0191	0.0775	0.110±0.0547
54b (E2)		27 (est.)	Nt	Nt
57	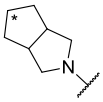	8.6 (est.)	Nt	Nt
60	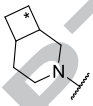	0.0365±0.00355	0.0389	Nt
62	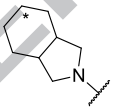	0.930	Nt	Nt
65	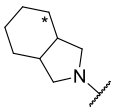	1.01	Nt	Nt
68	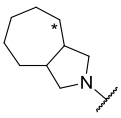	15 (est)	Nt	Nt
70	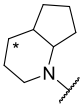	0.0511±0.00468	0.0366	Nt
70a (E1)		0.0284±0.00574	Nt	Nt
70b (E2)		0.189±0.0355	Nt	Nt
74	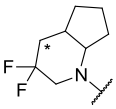	0.180±0.0148	Nt	Nt

76	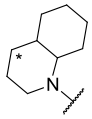	0.227±0.0429	Nt	Nt
79	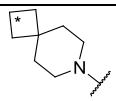	0.306±0.075	Nt	Nt
82	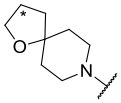	0.813	Nt	Nt
85		0.340±0.139	Nt	Nt
87	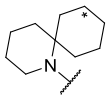	0.0863±0.0312	0.0881	0.0825±0.0337

[a] IC_{50} values are given as geometric means ±SEM of at least three independent experiments, each performed in quadruplicate (no SEM-values indicate a lower number of independent experiments).

[b] Replacement of [^{3}H]-M-MPEP; K_i values are given as geometric means ±SEM of at least three independent experiments each performed in triplicates.

Further modifications and variations of the nortropane core produced three different compound subseries grouped as bridged and fused bicyclic ring systems and spiro compounds (Table 2). For proper comparison with parent compound **1**, the original substitution pattern was not altered. Starting with nortropane derivative **9**, the bridge length within the bicyclic system as well as the position of the ring-nitrogen was varied. The switch from a [3.2.1] (**9**) to a [3.3.1] ring system in compound **39** had a detrimental effect on the mGluR5 activity, indicated by a 20-fold drop of the respective IC_{50}. However, when the positions of the ring nitrogen and the ethynyl substitution were interchanged, leading to compound **47**, the high potency of **9** was fully restored. Surprisingly, the shrinkage of the 3-carbon-bridge in compound **47** to a 2- or 1-carbon-bridge produced compounds (**45** and **42**, respectively) with only micromolar potencies. The same effect was observed when an oxygen was incorporated into the bridge, realized with compound **49** (hIC_{50} = 3.35 µM). On the other hand, compound **52a**, containing a [2.2.2] ring system, showed a hIC_{50} value below 100 nM, suggesting that certain flexibility in spatial size and orientation is given for the core structure. However, its OH-*endo* isomer **52b** was found to be almost inactive. Stereochemistry and particularly the specific orientation of the alkyne and the hydroxyl residues again seem to have a critical impact on receptor binding, like already seen with the compound pair **11a** and **11b**.

The usage of various fused bicyclic scaffolds, structurally derived from the core structure of AFQ-056 (**1**), led to the discovery of several potent analogs. Basically, both the position of the alkyne substituent as well as the size and orientation of the rings exerted an effect on activity on target. Although compounds **54** and **57** share the same hexahydrocyclopenta[*c*]pyrrole core structure, the determined activities were found to be significantly divergent. The eightyfold higher activity of **54** is obviously caused by the different ring attachment point of the ethinyl moiety and therefore by the discriminative shape of the two regioisomers, with the one of **54** being preferred. Consequently, its enantiomers **54a** and **54b** were isolated and tested separately. As a result, **54a** turned out to be 360-fold more potent as compared with its enantiomer **54b**, highlighting the great impact of the spatial orientation of the alkyne residue on receptor binding. Analog **60**, which contains a [6,4] ring system instead of a [5,5] bicycle, turned out to be one of the most active compounds. The racemic mixture showed an excellent hIC_{50} value of 0.0365 µM (respective enantiomers have not been separated). In contrast, a [5,6] ring system as substructure of compounds **62** and **65** were less effective, demonstrated by *in vitro* potencies around 1 µM. In this case, the position of the alkyne substitution had no effect on activity. Ring extension to a [5,7] bicycle like present in compound **68** was even more derogatory. Additional piperidine-based analogs as a follow-up of the highly active compound **60** proved to be more suitable, achieving activities in the two- and three-digit nanomolar range. In particular, one enantiomer of octahydro-1*H*-cyclopenta[*b*]pyridine derivative **70** (**70a**, absolute configuration unknown) convinced as the most active substance within the entire series (hIC_{50} = 0.0284 µM). Notably, the difference between the IC_{50} values measured for the two enantiomers was only sixfold as compared with a ratio of 360 obtained for **54a** and **54b**. With difluorinated analog **74** (hIC_{50} = 0.180 µM) – designed to improve the relatively low metabolic stability of **70** (*vide infra*) – the high potency could not be retained, unfortunately. The same range was hit with octahydroquinoline derivative **76**.

Ultimately, diverse spiro ring systems were introduced into the structure template. 4-, 5-, and 6-Membered rings were utilized as second cycle while the *N*-substituted pyridine ring was maintained in each case. The four presented examples **79**, **82**, **85**, and **87** all showed IC_{50} values in the submicromolar range, with azaspiro[5.5]undecane derivative **87** (hIC_{50} = 0.0863 µM) being the most potent member of this subseries.

In a next step, the most promising lead candidates were further characterized with respect to solubility in aqueous media and stability in human and rat liver microsomes (Table 3). While most of the tested compounds showed a solubility profile comparable to the data obtained for template compound **1**, particularly analogs **9** and **12**, two compounds with significantly divergent results were identified. On the one hand, the only compound devoid of the hydroxyl group (**35**) was found to be markedly less soluble, as expected. Due to the poor solubility in the assay medium compound **35** has therefore not been characterized further. On the other hand,

hexahydrocyclopenta[*c*]pyrrole derivative **54a** displayed a more than twofold higher solubility in both the *in vitro* assay medium and water (pH 7.4) as compared with AFQ-056 (**1**). Moreover, this compound also displayed an improved profile with respect to metabolic stability in human and rat liver microsomes. As a consequence, the fast and extensive metabolism of compound **1** observed in healthy subjects after single dose administration could potentially be positively modulated with compound **54a**.[17] In contrast, several structurally different candidates such as **21**, **22**, **47**, **70**, and **87** revealed a very poor metabolic stability, which led to an instant termination of further development. The observed instability could be reduced either to specific *N*-substituents like an ethyloxycarbonyl group in compound **21** – its methyl analog **9** proved to be markedly more stable – or to the specific type of the bicyclic scaffold, for example in spiro compound **87**, which ring system might be metabolically opened up. In general, metabolic stability was found to be noticeably higher in human than in rat liver microsomes for almost all tested compounds.

Table 3. Solubility and metabolic stability data

Compound ID	Solubility A[a] [µM]	Solubility B[b] [µg/mL]	CL_{int} (h/r)[c] (µL/min/mg)
1	190	26	51 / 134
6	440	19	33 / 314
8	Nt	Nt	69 / 266
9	274	24	68 / 458
11a	466	17	67 / 385
12	170	24	41 / 120
21	Nt	Nt	428 / 2718
22	Nt	Nt	141 / 889
35	6	Nt	Nt
47	Nt	Nt	155 / 983
52a	Nt	Nt	71 / 651
54a	470	60	28 / 54
60	Nt	Nt	30 / 139
70	Nt	Nt	278 / 1100
87	76	Nt	758 / 734

[a] Kinetic solubility in assay medium (0.5% DMSO/TRIS buffer).

[b] Thermodynamic solubility in water (pH = 7.4).

[c] Intrinsic clearance in human and rat liver microsomes.

In conclusion, we could show that based on the chemical structure of Novartis' clinical mGluR5 NAM AFQ-056 (Mavoglurant) various modifications of the bicyclic core structure were well tolerated by the receptor. By means of a scaffold hopping approach a diverse set of potent analogs structurally derived from fused or bridged bicyclic scaffolds or spiro compounds was generated. Most notably, compound **54a** not only showed equipotency on the mGlu5 receptor but also an improved aqueous solubility and metabolic stability profile as compared with AFQ-056, leveraging a further development and characterization *in vivo* to demonstrate safety and efficacy in the treatment of L-DOPA induced dyskinesia.

Acknowledgments

The authors warmly thank Andrea Baude, Sabine Falk and Christiane Reinbach for expert technical assistance in *in vitro* activity experiments, Dr. Meik Sladek for providing the *in vitro* binding data, Michelle Werner for ascertaining metabolic stability data, and Jens Neubauer and Kathleen Wolff for solubility determinations.

Supplementary data

Supplementary data (experimental details for the synthesis and characterization of intermediate and final products) associated with this article can be found, in the online version, at http://...

References and notes

1. Petroff, O. A. *The Neuroscientist : a review journal bringing neurobiology, neurology and psychiatry* **2002,** *8*, 562.
2. Jaeschke, G.; Wettstein, J. G.; Nordquist, R. E.; Spooren, W. *Expert Opinion on Therapeutic Patents* **2008,** *18*, 123.
3. Pin, J. P.; Kniazeff, J.; Liu, J.; Binet, V.; Goudet, C.; Rondard, P.; Prezeau, L. *The FEBS journal* **2005,** *272*, 2947.
4. Crawford, J. H.; Wainwright, A.; Heavens, R.; Pollock, J.; Martin, D. J.; Scott, R. H.; Seabrook, G. R. *Neuropharmacology* **2000,** *39*, 621.
5. Gross, C.; Berry-Kravis, E. M.; Bassell, G. J. *Neuropsychopharmacology : official publication of the American College of Neuropsychopharmacology* **2012,** *37*, 178.
6. Berg, D.; Godau, J.; Trenkwalder, C.; Eggert, K.; Csoti, I.; Storch, A.; Huber, H.; Morelli-Canelo, M.; Stamelou, M.; Ries, V.; Wolz, M.; Schneider, C.; Di Paolo, T.; Gasparini, F.; Hariry, S.; Vandemeulebroecke, M.; Abi-Saab, W.; Cooke, K.; Johns, D.; Gomez-Mancilla, B. *Movement disorders : official journal of the Movement Disorder Society* **2011,** *26*, 1243.
7. Zerbib, F.; Bruley des Varannes, S.; Roman, S.; Tutuian, R.; Galmiche, J. P.; Mion, F.; Tack, J.; Malfertheiner, P.; Keywood, C. *Alimentary pharmacology & therapeutics* **2011,** *33*, 911.
8. Keywood, C.; Wakefield, M.; Tack, J. *Gut* **2009,** *58*, 1192.
9. Ribeiro, F.; Pires, R. W.; Ferguson, S. G. *Mol Neurobiol* **2011,** *43*, 1.
10. Grégoire, L.; Morin, N.; Ouattara, B.; Gasparini, F.; Bilbe, G.; Johns, D.; Vranesic, I.; Sahasranaman, S.; Gomez-Mancilla, B.; Di Paolo, T. *Parkinsonism & Related Disorders* **2011,** *17*, 270.
11. Rocher, J.-P.; Bonnet, B.; Bolea, C.; Lutjens, R.; Le Poul, E.; Poli, S.; Epping-Jordan, M.; Bessis, A.-S.; Ludwig, B.; Mutel, V. *Current Topics in Medicinal Chemistry* **2011,** *11*, 680.
12. Emmitte, K. A. *ACS Chemical Neuroscience* **2011,** *2*, 411.
13. Lovering, F.; Bikker, J.; Humblet, C. *Journal of Medicinal Chemistry* **2009,** *52*, 6752.
14. Abel, U. WO2012152854; **2012**.
15. Müller, S.; Liepold, B.; Roth, G. J.; Bestmann, H. J. *Synlett* **1996,** *1996*, 521.
16. Sonogashira, K. *Journal of Organometallic Chemistry* **2002,** *653*, 46.
17. Walles, M.; Wolf, T.; Jin, Y.; Ritzau, M.; Leuthold, L. A.; Krauser, J.; Gschwind, H.-P.; Carcache, D.; Kittelmann, M.; Ocwieja, M.; Ufer, M.; Woessner, R.; Chakraborty, A.; Swart, P. *Drug Metabolism and Disposition* **2013,** *41*, 1626.

Table 1. mGluR5 *in vitro* potency data of azabicyclo[3.2.1]octane derivatives

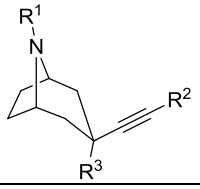

Compound ID	R^1	R^2	R^3	Human mGluR5 (CHO) IC_{50} (μM)[a]	Rat mGluR5 (rpA) IC_{50} (μM)[a]	Rat mGluR5 (CHO) [^{3}H]-M-MPEP K_i (μM)[b]
1 (AFQ-056)	-	-	-	0.0716±0.00647	0.0516±0.00595	0.0660±0.00624
5			OH	0.298±0.0248	Nt	Nt
6		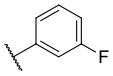	OH	0.0613±0.0091	0.0678±0.00489	0.0777±0.00577
7		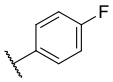	OH	2.19	Nt	Nt
8		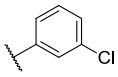	OH	0.0274±0.00296	0.0252	Nt
9		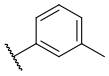	OH	0.0507±0.00579	0.0479±0.00583	0.0710
10		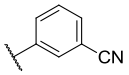	OH	0.187±0.0282	Nt	Nt
11a		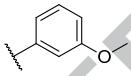	OH	0.0763±0.00877	0.0740	0.0760
12		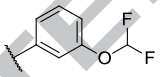	OH	0.0722±0.0142	0.0907	0.0578±0.00612
14		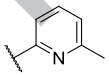	OH	0.818	Nt	Nt
15		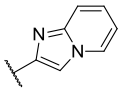	OH	>100	Nt	Nt
19		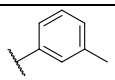	OH	0.543	Nt	Nt
20		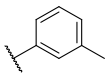	OH	0.308±0.00664	Nt	Nt
21	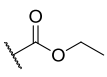	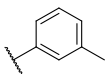	OH	0.0478±0.00247	0.0291	Nt
22		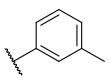	OH	0.132±0.0172	0.113	Nt
24		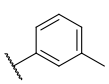	OH	0.210±0.0219	Nt	Nt
27	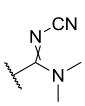	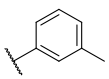	OH	0.168±0.0150	Nt	Nt

29		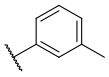	OH	0.575	Nt	Nt
31		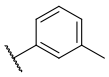	OH	0.170±0.0248	Nt	Nt
35		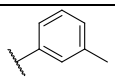	H	0.0648±0.0140	Nt	Nt
36		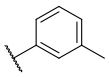	OMe	0.137±0.0264	Nt	Nt

[a] IC_{50} values are given as geometric means ±SEM of at least three independent experiments, each performed in quadruplicate (no SEM-values indicate a lower number of independent experiments).

[b] Replacement of [^{3}H]-M-MPEP; K_i values are given as geometric means ±SEM of at least three independent experiments each performed in triplicates.

Table 2. mGluR5 *in vitro* potency data of further AFQ-056 analogs

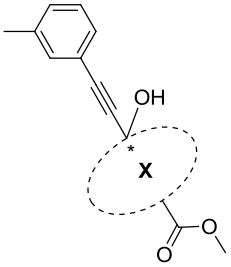

Compound ID	X	Human mGluR5 (CHO) IC_{50} (μM)[a]	Rat mGluR5 (rpA) IC_{50} (μM)[a]	Rat mGluR5 (ctx) [^{3}H]-M-MPEP K_i (μM)[b]
1 (AFQ-056)	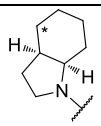	0.0716±0.00647	0.0516±0.00595	0.0660±0.00624
9		0.0507±0.00579	0.0479±0.00583	0.0710
39		1.02	Nt	Nt
42		5.0 (est.)	Nt	Nt
45		49 (est.)	Nt	Nt
47	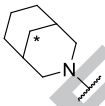	0.0466±0.0055	0.0325	Nt
49	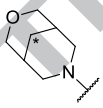	3.35	Nt	Nt
52a (*exo*-OH)		0.0850±0.00613	0.0387	Nt
52b (*endo*-OH)		52 (est.)	Nt	Nt
54 (*rac*)	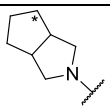	0.103±0.0169	0.188±0.0274	Nt
54a (E1)		0.0748±0.0191	0.0775	0.110±0.0547
54b (E2)		27 (est.)	Nt	Nt
57	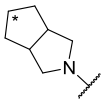	8.6 (est.)	Nt	Nt
60	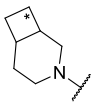	0.0365±0.00355	0.0389	Nt
62	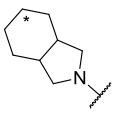	0.930	Nt	Nt
65	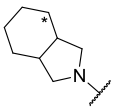	1.01	Nt	Nt

68	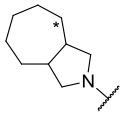	15 (est)	Nt	Nt
70	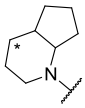	0.0511±0.00468	0.0366	Nt
70a (E1)		0.0284±0.00574	Nt	Nt
70b (E2)		0.189±0.0355	Nt	Nt
74	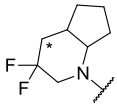	0.180±0.0148	Nt	Nt
76	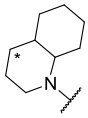	0.227±0.0429	Nt	Nt
79	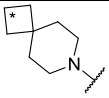	0.306±0.075	Nt	Nt
82	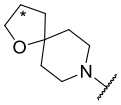	0.813	Nt	Nt
85		0.340±0.139	Nt	Nt
87	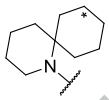	0.0863±0.0312	0.0881	0.0825±0.0337

[a] IC_{50} values are given as geometric means ±SEM of at least three independent experiments, each performed in quadruplicate (no SEM-values indicate a lower number of independent experiments).

[b] Replacement of [^{3}H]-M-MPEP; K_i values are given as geometric means ±SEM of at least three independent experiments each performed in triplicates.

Table 3. Solubility and metabolic stability data

Compound ID	Solubility A[a] [µM]	Solubility B[b] [µg/mL]	CL_{int} (h/r)[c] (µL/min/mg)
1	190	26	51 / 134
6	440	19	33 / 314
8	Nt	Nt	69 / 266
9	274	24	68 / 458
11a	466	17	67 / 385
12	170	24	41 / 120
21	Nt	Nt	428 / 2718
22	Nt	Nt	141 / 889
35	6	Nt	Nt
47	Nt	Nt	155 / 983
52a	Nt	Nt	71 / 651
54a	470	60	28 / 54
60	Nt	Nt	30 / 139
70	Nt	Nt	278 / 1100
87	76	Nt	758 / 734

[a] Kinetic solubility in assay medium (0.5% DMSO/TRIS buffer).

[b] Thermodynamic solubility in water (pH = 7.4).

[c] Intrinsic clearance in human and rat liver microsomes.

Figure 1

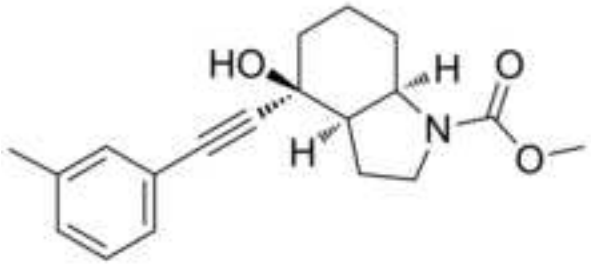

AFQ-056 (**1**)
(Mavoglurant, Novartis)

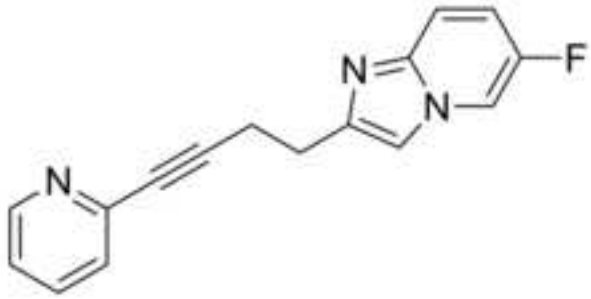

ADX-48621 (**2**)
(Dipraglurant, Addex)

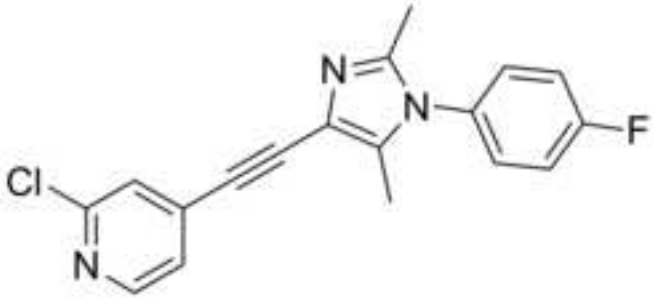

RG-7090 (**3**)
(Roche)

Figure 2

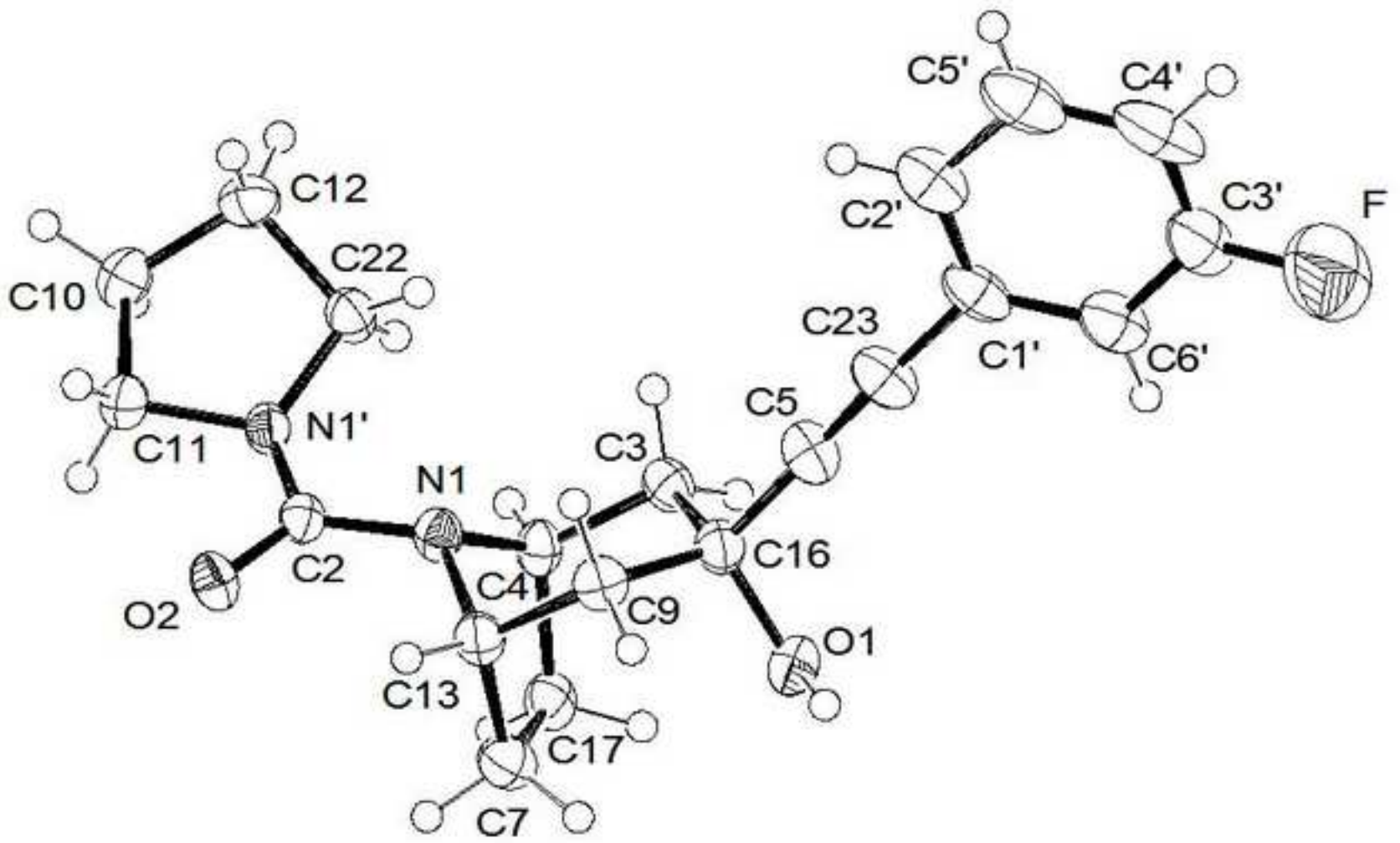

Scheme 1

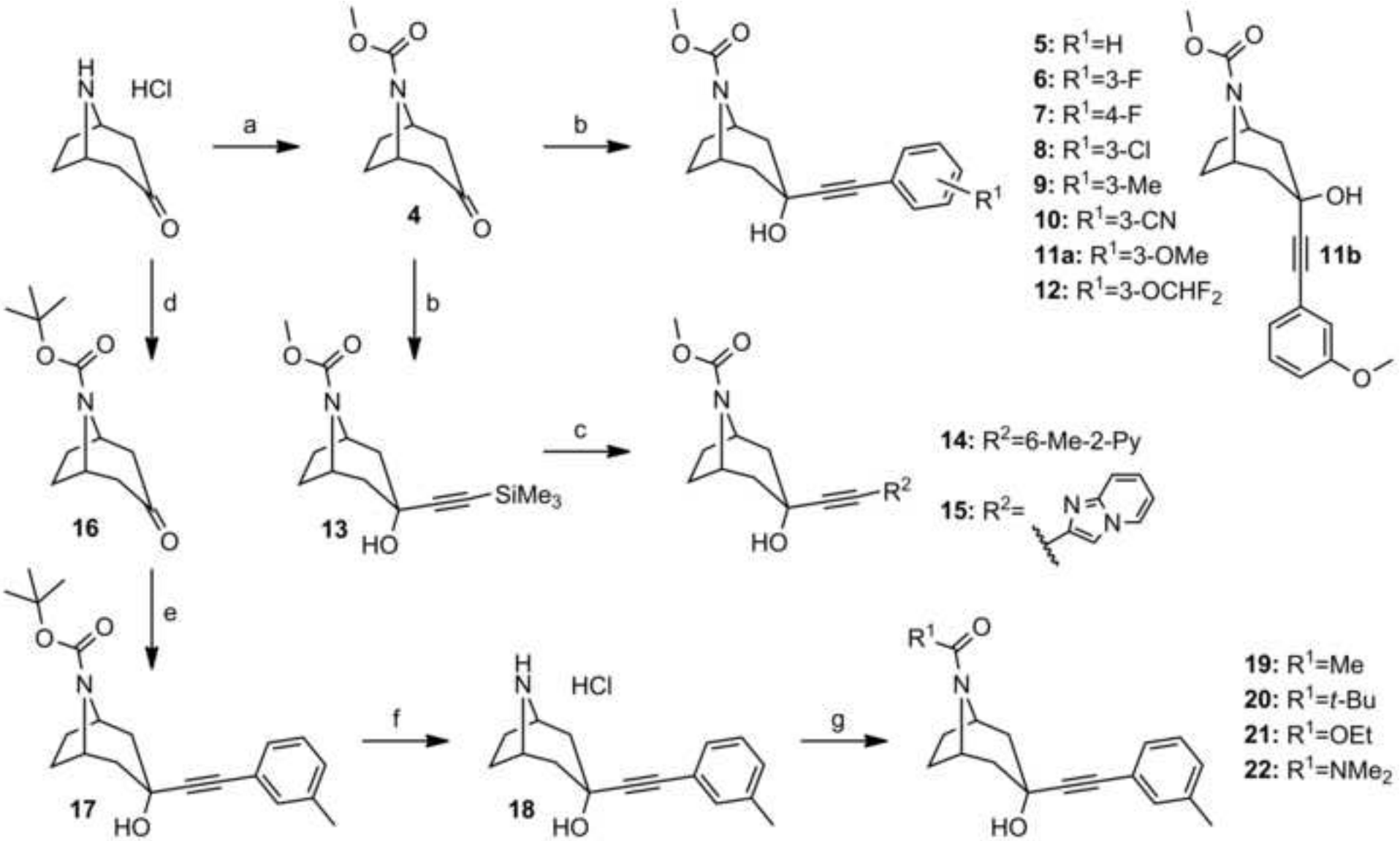

Scheme 2

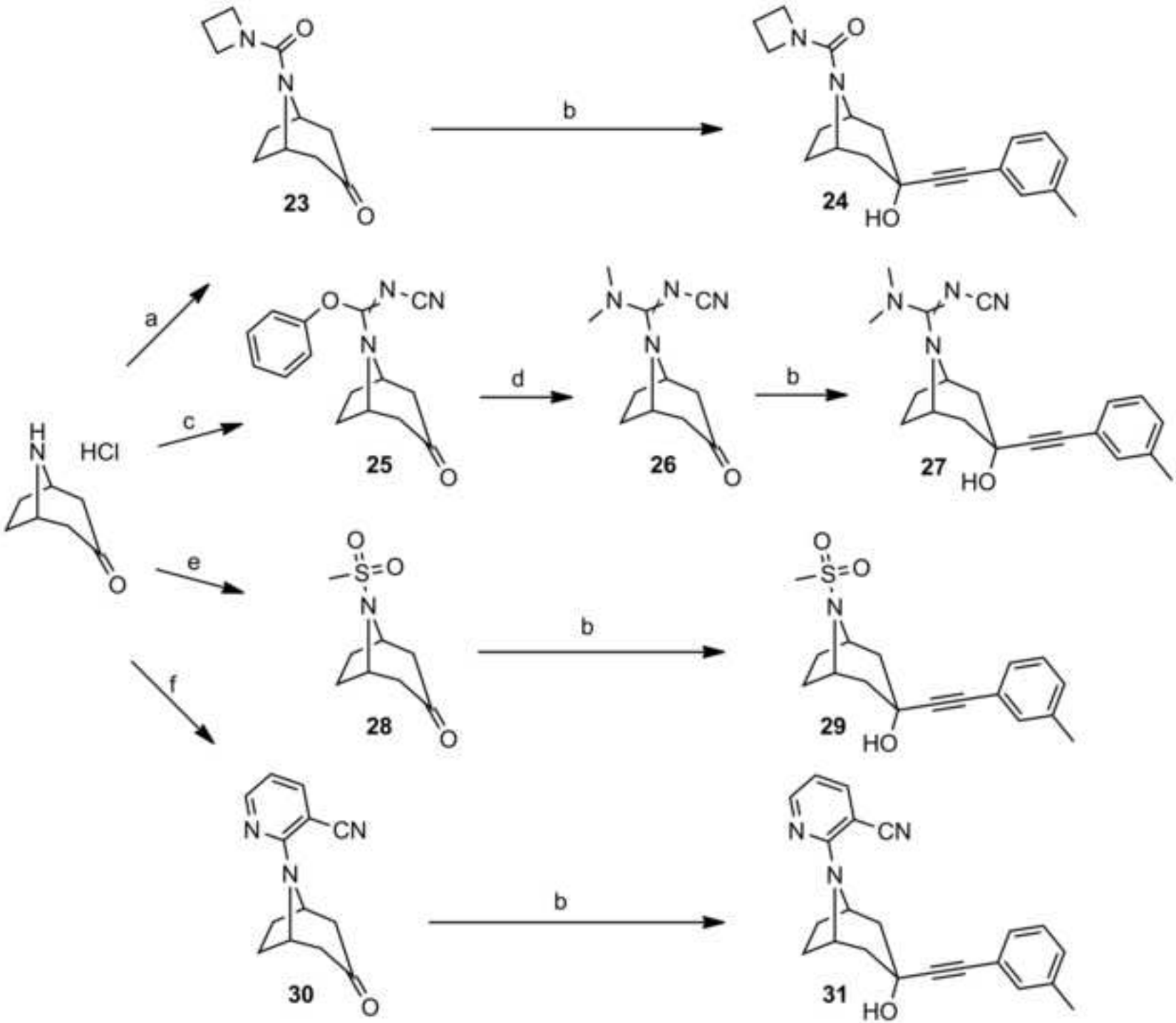

Scheme 3

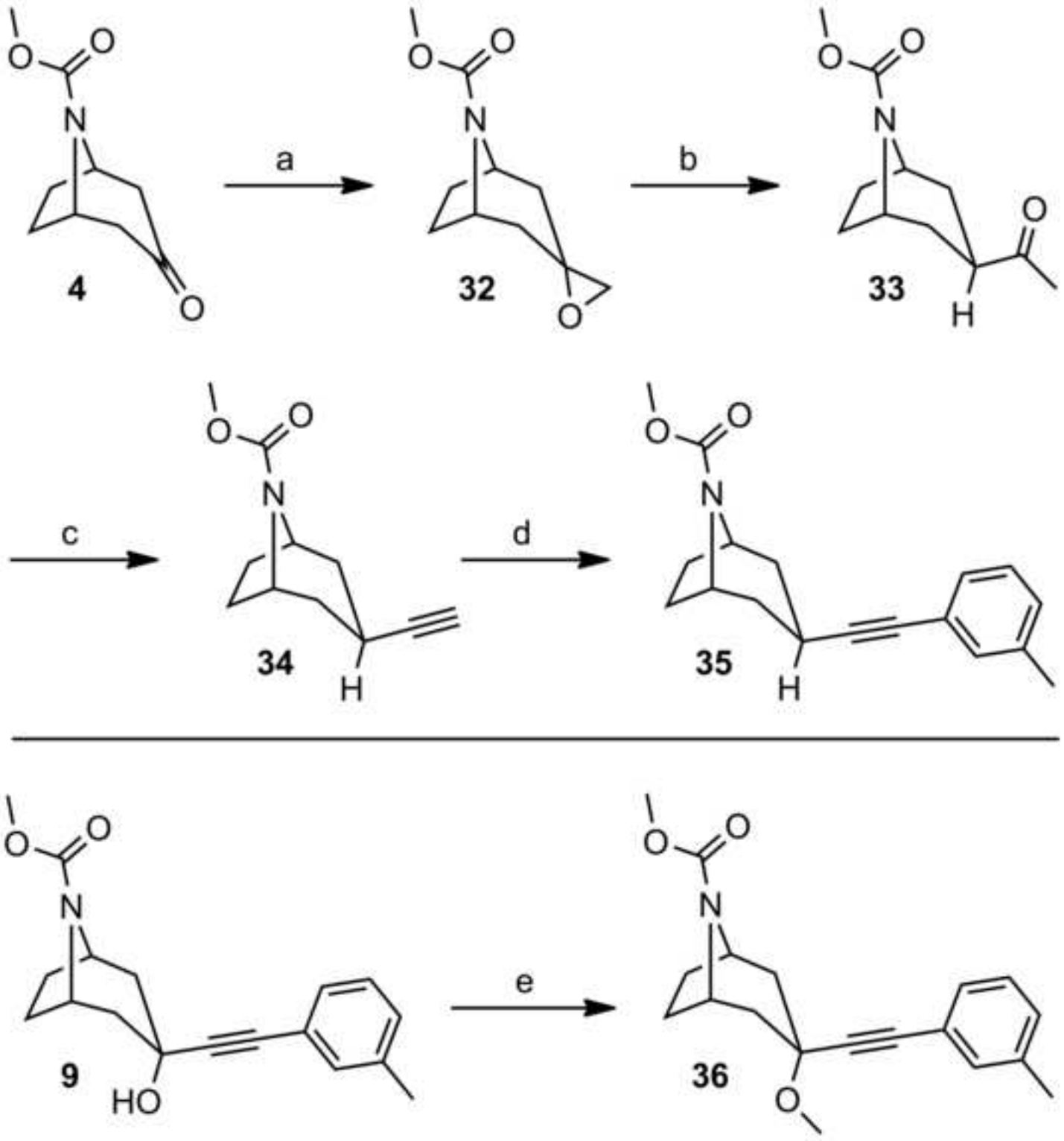

Scheme 4

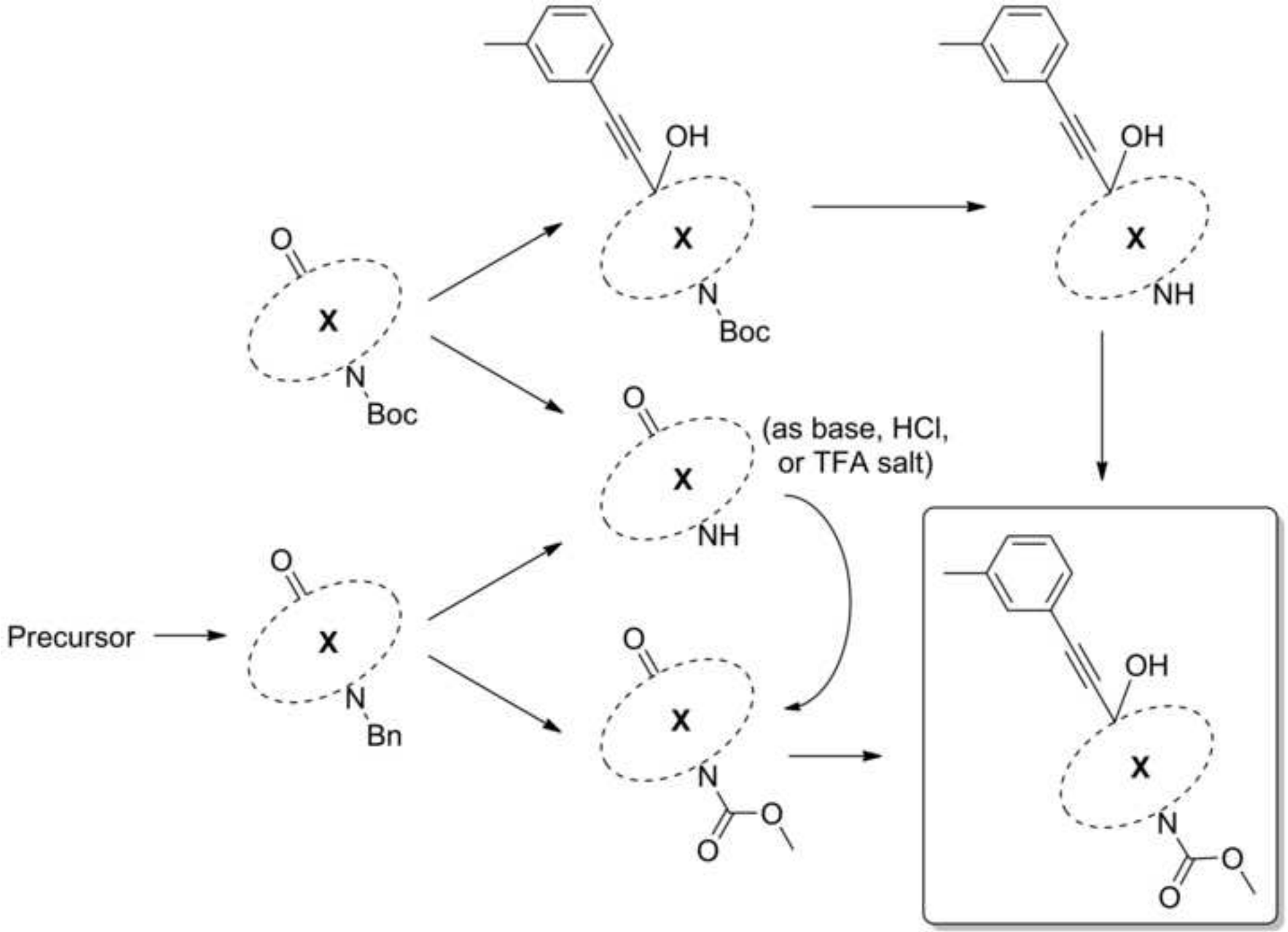

Captions

Figure 1. Clinically evaluated mGluR5 negative allosteric modulators.

Figure 2. Crystal structure of 3-((3-fluorophenyl)ethynyl)-3-*endo*-hydroxy-8-azabicyclo[3.2.1]octan-8-yl)(pyrrolidin-1-yl)methanone (**I**).

Scheme 1. Reagents and conditions: (a) methyl chloroformate, Et_3N, DMAP, THF, rt, 3 h; (b) 1. subst. ethyne, *n*-BuLi, THF, -20 $^oC \rightarrow 0\ ^oC$, 90 min; 2. **4**, THF, -78 $^oC \rightarrow$ 0–5 ^oC, 2 h; (c) aryl halide, Et_3N, DMF, CuI, $PdCl_2(PPh_3)_2$, TBAF, THF, 60 ^oC, 2 h → rt, overnight; (d) di-*tert*-butyl dicarbonate, Et_3N, DMAP, DCM, 0 $^oC \rightarrow$ rt, 16 h; (e) 1. 1-ethynyl-3-methylbenzene, *n*-BuLi, THF, -20 $^oC \rightarrow 0\ ^oC$, 1 h; 2. **16**, THF, -20 $^oC \rightarrow 0\ ^oC$; 1h; (f) 4N HCl in dioxane, DCM, rt, 1h; (g) R-C(O)Cl, Et_3N, DCM, 0 $^oC \rightarrow$ rt, overnight.

Scheme 2. Reagents and conditions: (a) 1. diphosgene, DCM, rt, 30 min; 2. azetidine, Et_3N, rt, 1 h; (b) 1. 1-ethynyl-3-methylbenzene, *n*-BuLi, THF, -20 $^oC \rightarrow 0\ ^oC$, 90 min; 2. **23**, **26**, **28**, or **30**, resp., THF, -78 $^oC \rightarrow$ 0–5 ^oC, 2 h; (c) diphenyl cyanocarbonimidate, Et_3N, DCM, rt, 2 h; (d) Et_2NH/THF, iPrOH, 80 ^oC, 3 h; (e) methylsulfonyl chloride, DIPEA, DCM, rt, 4 h; (f) 2-chloronicotinonitrile, Et_3N, THF, reflux, 3 days.

Scheme 3. Reagents and conditions: (a) 1. trimethylsulfoxonium iodide, KOtBu, THF, N_2, reflux, 3 h; 2. **4**, THF, rt, 3 days; (b) 1. **32**, $BF_3 \times Et_2O$, THF, -3 $^oC \rightarrow 5\ ^oC$; 3 h, rt, overnight; 2. DBU, MeOH, THF, rt, 1 h; (c) dimethyl 1-diazo-2-oxopropylphosphonate, K_2CO_3, MeOH, 0 $^oC \rightarrow$ rt, 2 h; (d) 1-iodo-3-methylbenzene, $Pd(PPh_3)_4$, CuI, Et_3N, DMF, N_2, 60 ^oC, 1 h; (e) *n*-BuLi (1.6M in hexanes), MeI, THF, DMSO, -78 ^oC, 1.5 h.

Scheme 4. General synthesis routes towards final products **39**, **42**, **45**, **47**, **49**, **52a**, **52b**, **54**, **54a**, **54b**, **57**, **60**, **62**, **65**, **68**, **70**, **70a**, **70b**, **74**, **76**, **79**, **82**, **85**, and **87**. For details please refer to the Supplementary material.

Table 1. mGluR5 *in vitro* potency data of azabicyclo[3.2.1]octane derivatives

Table 2. mGluR5 *in vitro* potency data of further AFQ-056 analogs